Astrofisica Generale II — 6

Maurizio Tomasi (maurizio.tomasi@unimi.it)

28 Marzo 2025

Jeans' Collapse

These are the equations used by Jeans:

$$\dot{\rho} + \vec{\nabla}\left(\rho\,\vec{v}\right) = 0 \qquad \text{(mass conservation)}$$

$$\dot{\vec{v}} + (\vec{v}\cdot\nabla)\vec{v} = -\frac{1}{\rho}\vec{\nabla}p - \vec{\nabla}\phi \qquad \text{(Newton's law)}$$

$$p = \rho c_s^2 \qquad \text{(speed of sound)}$$

$$\nabla^2\phi = 4\pi G\rho \qquad \text{(gravitation).}$$

The unknowns $\rho, \vec{v}, p$ and ϕ are functions of the point $\vec{r}$ and time t. For a monoatomic ideal gas, $c_s = \sqrt{\gamma\frac{k_B T}{m}}$, with $\gamma = \frac{5}{3}$.

Jeans' Derivation

- The system of equations is very complex to solve without some simplification.
- We linearize the system, substituting

$$\rho(\vec{r},t) = \rho_0 + \rho_1(\vec{r},t),$$
$$p(\vec{r},t) = p_0 + p_1(\vec{r},t),$$
$$\vec{v}(\vec{r},t) = \vec{v}_0 + \vec{v}_1(\vec{r},t) = 0 + \vec{v}_1(\vec{r},t),$$
$$\phi(\vec{r},t) = \phi_0 + \phi_1(\vec{r},t).$$

The terms $\rho_0, p_0, \vec{v}_0$ and ϕ_0 are constant, and $\rho_0 \gg \rho_1, p_0 \gg p_1$, etc.

Jeans' Derivation

Ignoring higher-order terms, we have that, for example, the term $-\vec{\nabla}p/\rho$ becomes

$$-\frac{1}{\rho}\vec{\nabla}p = -\frac{\vec{\nabla}p_1}{\rho_0+\rho_1} \approx -\frac{\vec{\nabla}p_1}{\rho_0}\left(1-\frac{\rho_1}{\rho_0}\right) =$$

$$= -\frac{\vec{\nabla}p_1}{\rho_0} + \frac{\rho_1}{{\rho_0}^2}\vec{\nabla}p_1 \approx -\frac{\vec{\nabla}p_1}{\rho_0}.$$

The remaining terms are simpler.

Jeans' derivation

- Applying a divergence to the so-called «Newton's law» and substituting, we obtain

$$\ddot{\rho}_1 - c_s^2 \nabla^2 \rho_1 + 4\pi G \rho_1 \rho_0 = 0.$$

- The equation is complex to solve, but it is linear: if ρ_A and ρ_B are two solutions, then $\alpha\rho_A + \beta\rho_B$ is also a solution.

Jeans' derivation

We exploit the linearity of the equation to solve it using Fourier analysis. We therefore decompose the unknown into plane waves:

$$\rho_1(\vec{r},t) = \iiint_{\mathbb{R}^3} \mathrm{d}\vec{k} \int_{\mathbb{R}} \mathrm{d}\omega\, \tilde{\rho}_1(\vec{k},\omega)\, e^{i(\vec{k}\cdot\vec{r}-\omega t)}.$$

The function $\tilde{\rho}_1(\vec{k},\omega)$ is the Fourier transform of $\rho_1(\vec{r},t)$; therefore differential operations on ρ_1 become algebraic on $\tilde{\rho}_1$:

$$\nabla^2\rho_1 \to k^2 \cdot \tilde{\rho}_1, \qquad \partial_t\rho_1 \to \omega \cdot \tilde{\rho}_1.$$

Jeans' derivation

Recalling that

$$\left\|\vec{k}\right\| = \frac{2\pi}{\lambda}, \quad \omega = 2\pi\nu,$$

the value of λ that appears in the expression of ρ_1 corresponds each time to a different scale of the perturbations in the image:

Jeans' derivation

Therefore, applying the Fourier transform to the equation of ρ_1, we obtain

$$\omega^2 \cdot \tilde{\rho}_1 = \left(k^2 c_s^2 - 4\pi G \rho_0\right) \cdot \tilde{\rho}_1,$$

that is

$$\omega^2 = k^2 c_s^2 - 4\pi G \rho_0,$$

which is called the **dispersion relation** and links ω and k (i.e., λ and ν).

Jeans' derivation

- The solution is

$$\omega = \pm c_s \sqrt{k^2 - k_J^2}, \quad k_J^2 \equiv \frac{4\pi G \rho_0}{c_s^2}.$$

  (in the absence of gravity, $k_J = 0$ and $\omega = \pm c_S\, k$: the speed of sound is always c_s).

- From the study of this equation, we deduce how the system evolves over time.

Jeans' derivation

If $k_J^2 < k^2$ then the pressure wave propagates in the medium (acoustic wave) with a phase velocity given by

$$v_f = \lambda\nu = \frac{\omega}{k} = c_s\sqrt{1 - \left(\frac{k_J}{k}\right)^2},$$

lower than the speed of sound c_s because $k_J \neq 0$ (it is the term due to gravity). Gravity therefore «slows down» the propagation of the wave in the medium.

Jeans' derivation

If $k_J^2 > k^2$ then ω is imaginary, and $\rho_1(\vec{r}, t) = A_g e^{i(\vec{k}\cdot\vec{r} - \omega t)}$ diverges as e^{t/τ_J} (collapse), with

$$\tau_J = \frac{1}{k_J c_s} = \frac{1}{\sqrt{4\pi G \rho_0}} = \frac{2.3 \times 10^4\,\mathrm{yr}}{\sqrt{n_H / 10^6\,\mathrm{cm}^{-3}}},$$

if $k \ll k_J$; a result similar to the *free-fall* time:

$$\tau_{\mathrm{ff}} = \sqrt{\frac{3\pi}{32 G \rho_0}} = \frac{4.4 \times 10^4\,\mathrm{yr}}{\sqrt{n_H / 10^6\,\mathrm{cm}^{-3}}}.$$

Jeans' derivation

Since the collapse occurs if $k_J^2 > k^2$, that is

$$\frac{4\pi G\rho_0}{c_s^2} > \left(\frac{2\pi}{\lambda}\right)^2,$$

we then obtain the expression for R_J:

$$\lambda > c_s\sqrt{\frac{\pi}{G\rho_0}} \equiv R_J.$$

For a monatomic gas we have $R_J = \sqrt{\frac{5\pi k_B T}{3Gm\rho_0}}$.

Jeans' mass

From the density ρ_0 and the Jeans radius R_J we can estimate the minimum mass to cause a gravitational collapse with

$$M_J = \frac{4}{3}\pi R_J^3 \rho_0 = \frac{4\pi}{3\sqrt{\rho_0}} \left(\frac{5\pi k_B T}{3Gm} \right)^{\frac{3}{2}} \propto \sqrt{\frac{T^3}{\rho_0}}$$

(«Jeans mass»).

Jeans' mass

Numerically, it holds that

$$M_J \approx 0.32\, M_\odot \left(\frac{T}{10\,\mathrm{K}}\right)^{\frac{3}{2}} \left(\frac{m_H}{\mu}\right)^{\frac{3}{2}} \left(\frac{n_0}{10^6\,\mathrm{cm}^3}\right)^{-\frac{1}{2}}$$

with μ average molecular weight.

The values of n and T in the equation are quite in line with those of the clouds in the ISM: this is reassuring!

Jeans' swindle

- We mentioned a physical problem in Jeans' calculations. The point is that it is unrealistic to assume that

$$\nabla \phi_0 = 0$$

  because then

$$\nabla^2 \phi_0 = 0 \quad \Rightarrow \quad 4\pi G \rho_0 = 0.$$

- Without the assumption $\nabla \phi = 0$, the calculations become more complicated, but the result does not change qualitatively.
- The correct solution, however, depends on the details of the geometry of the

Cloud Collapse Mechanisms

Jeans' Mass

- When very massive clouds begin to collapse, the physical parameters change, and so does M_J.
- In some cases, it may happen that some regions of the cloud lose stability and begin to collapse in turn. A **fragmentation** of the cloud occurs, with the formation of multiple stars.
- This is the likely mechanism for the formation of open clusters.

Cloud Rotation

- In general, a collapsing cloud will also have angular momentum, which we have neglected.
- If angular momentum is conserved during contraction, then:

$$\frac{2}{5}MR^2\omega = \frac{2}{5}MR_0^2\omega_0,$$

(the moment of inertia is $I = \frac{2}{5}MR^2$ for a solid sphere) from which

$$\omega = \omega_0 \left(\frac{R_0}{R}\right)^2.$$

Cloud Rotation

- At the equator, the acceleration is

$$a(R) = G\frac{M(R)}{R^2} - \omega^2 R = G\frac{M(R)}{R^2} - \omega_0^2 \left(\frac{R_0}{R}\right)^4 R.$$

- The rotation will stop the collapse when $a(R) = 0$, i.e.,

$$GM(R) = (\omega_0 R_0)^2 \frac{R_0^2}{R},$$

which occurs when $\frac{R}{R_0} = \frac{(\omega_0 R_0)^2 R_0}{GM(R)}$.

Cloud Rotation

- For typical values of $\omega_0 R_0 = 1\,\mathrm{km/s} = 10^5\,\mathrm{cm/s}$ and of M_J and R_J, it holds that

$$\frac{R}{R_0} \approx 0.6.$$

- Therefore, when the radius has reduced by half, the rotation slows the collapse in the direction $\perp$ to the axis of rotation.
- In the direction parallel to the axis, the collapse can continue undisturbed. The cloud flattens and forms a disk, where much of the mass does not reach the center and does not form the star.

Where Do Stars Form?

- Let's estimate the Jeans radius ($R_J \propto \sqrt{T/\rho}$) in two distinct cases:

  1. H_2 molecular cloud: $T \sim 10\,\mathrm{K}, n \sim 10^3\,\mathrm{cm}^{-3}$.
  2. HI cloud: $T \sim 100\,\mathrm{K}, n \sim 1\,\mathrm{cm}^{-3}$.

- We have that

$$\frac{R_{\mathrm{J,\,HI}}}{R_{\mathrm{J,\,H_2}}} \sim 2\sqrt{\frac{100\,\mathrm{K}}{10\,\mathrm{K}}\,\frac{10^3\,\mathrm{cm}^{-3}}{1\,\mathrm{cm}^{-3}}} = 200.$$

- It is therefore easier to form stars in **molecular clouds**.

Star Formation

- The collapse releases gravitational energy which can:

  1. increase the internal energy, modifying the pressure;
  2. be radiated outwards if the cooling time is less than τ_{ff}.

- In the second case, the contraction is isothermal. (This was Jeans' hypothesis, from which, in the case of small oscillations, the relation $p = \rho c_s^2$ that we used last time is derived).

Star Formation

- But the increase in ρ corresponds to an increase in the optical depth of the cloud, and at some point the collapse ceases to be isothermal, becoming adiabatic:

$$TV^{\gamma-1} = \text{constant} \quad \Rightarrow \quad T \propto \frac{1}{V^{\gamma-1}} \propto \rho^{\gamma-1}.$$

- Consequently,

$$M_J \propto \sqrt{\frac{T^3}{\rho}} \propto \sqrt{\rho^{3\gamma-4}}.$$

Star Formation

$$M_J \propto \sqrt{\rho^{3\gamma-4}}.$$

- If γ > 4/3 (e.g., ideal gas), M_J increases as density increases, and therefore the collapse could stop before nuclear reactions are triggered inside the star.
- When this happens, the Jeans mass for a 10^2 K cloud is about 0.2 $M_\odot$: therefore the process allows the formation of **a series of masses of the order of the solar mass**, but not much lower.

Photoionization

- If in the adiabatic regime the energy is not released outside the cloud, where does it go?
- Partly it is used to increase the temperature T, partly to photoionize the neutral species (H, He, H_2).
- This determines the path of the protostar on the HR diagram.

Cloud Contraction

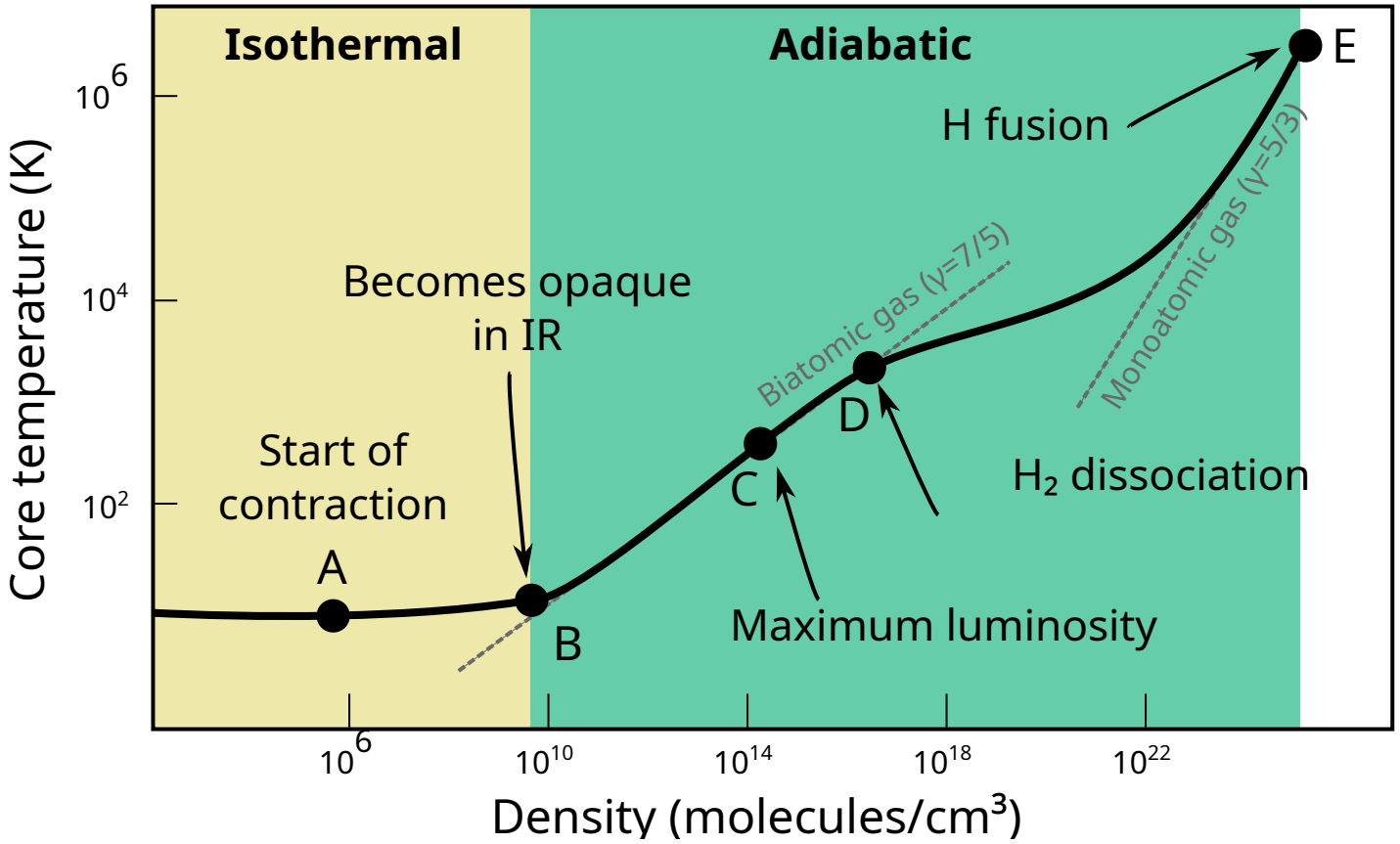

Numerical model of the collapse from a cloud to a protostar $M \sim 1\, M_\odot$.

Sites of Star Formation

As already mentioned, to identify H_2 regions we can use CO as a tracer:

1. The CO column density is estimated from the emission of rotational lines;
2. The H_2 column density is derived through an «X-factor»; see Bolatto, Wolfire & Leroy, Annu. Rev. Astron. Astrophys. 2013. 51:207–68 for a review.

CO Map (Planck 2013)

A&A 571, A13 (2014)
DOI: 10.1051/0004-6361/201321553

Planck 2013 results

Astronomy & Astrophysics

Special feature

Planck 2013 results. XIII. Galactic CO emission

Received 22 March 2013 / Accepted 21 March 2014

ABSTRACT

Rotational transition lines of CO play a major role in molecular radio astronomy as a mass tracer and in particular in the study of star formation and Galactic structure. Although a wealth of data exists for the Galactic plane and some well-known molecular clouds, there is no available high sensitivity all-sky survey of CO emission to date. Such all-sky surveys can be constructed using the *Planck* HFI data because the three lowest CO rotational transition lines at 115, 230 and 345 GHz significantly contribute to the signal of the 100, 217 and 353 GHz HFI channels, respectively. Two different component separation methods are used to extract the CO maps from *Planck* HFI data. The maps obtained are then compared to one another and to existing external CO surveys. From these quality checks the best CO maps, in terms of signal to noise ratio and/or residual contamination by other emission, are selected. Three different sets of velocity-integrated CO emission maps are produced with different trade-offs between signal-to-noise, angular resolution, and reliability. Maps for the CO $J = 1 \rightarrow 0$, $J = 2 \rightarrow 1$, and $J = 3 \rightarrow 2$ rotational transitions are presented and described in detail. They are shown to be fully compatible with previous surveys of parts of the Galactic plane as well as with undersampled surveys of the high latitude sky. The *Planck* HFI velocity-integrated CO maps for the $J = 1 \rightarrow 0$, $J = 2 \rightarrow 1$, and $J = 3 \rightarrow 2$ rotational transitions provide an unprecedented all-sky CO view of the Galaxy. These maps are also of great interest to monitor potential CO contamination of the *Planck* studies of the cosmological microwave background.

Key words. ISM: molecules

CO Map (Planck 2013)

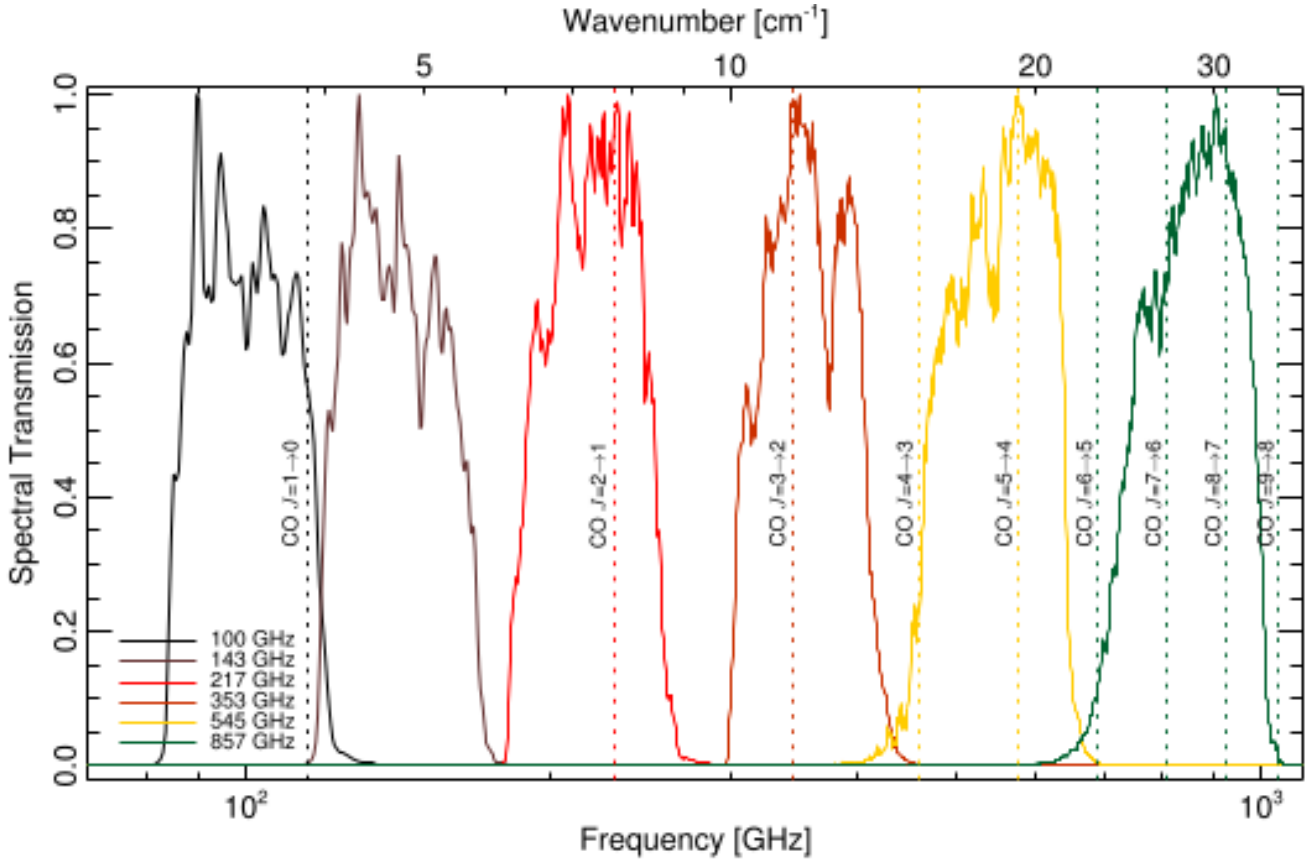

Fig. 1. The average spectral response for each of the HFI frequency bands. The vertical bars represent the CO rotational transitions.

CO Map (Planck 2013)

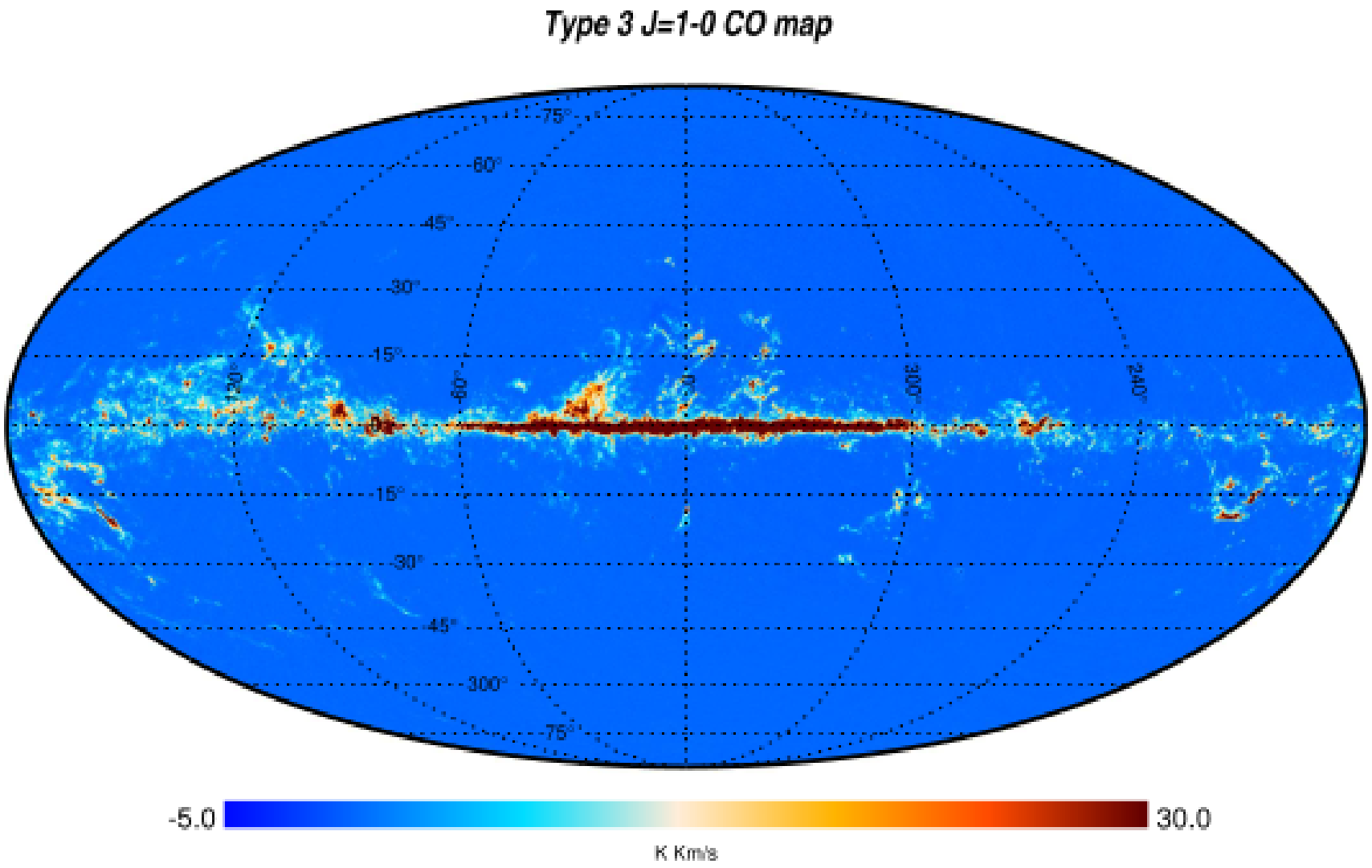

CO Map (Planck 2013)

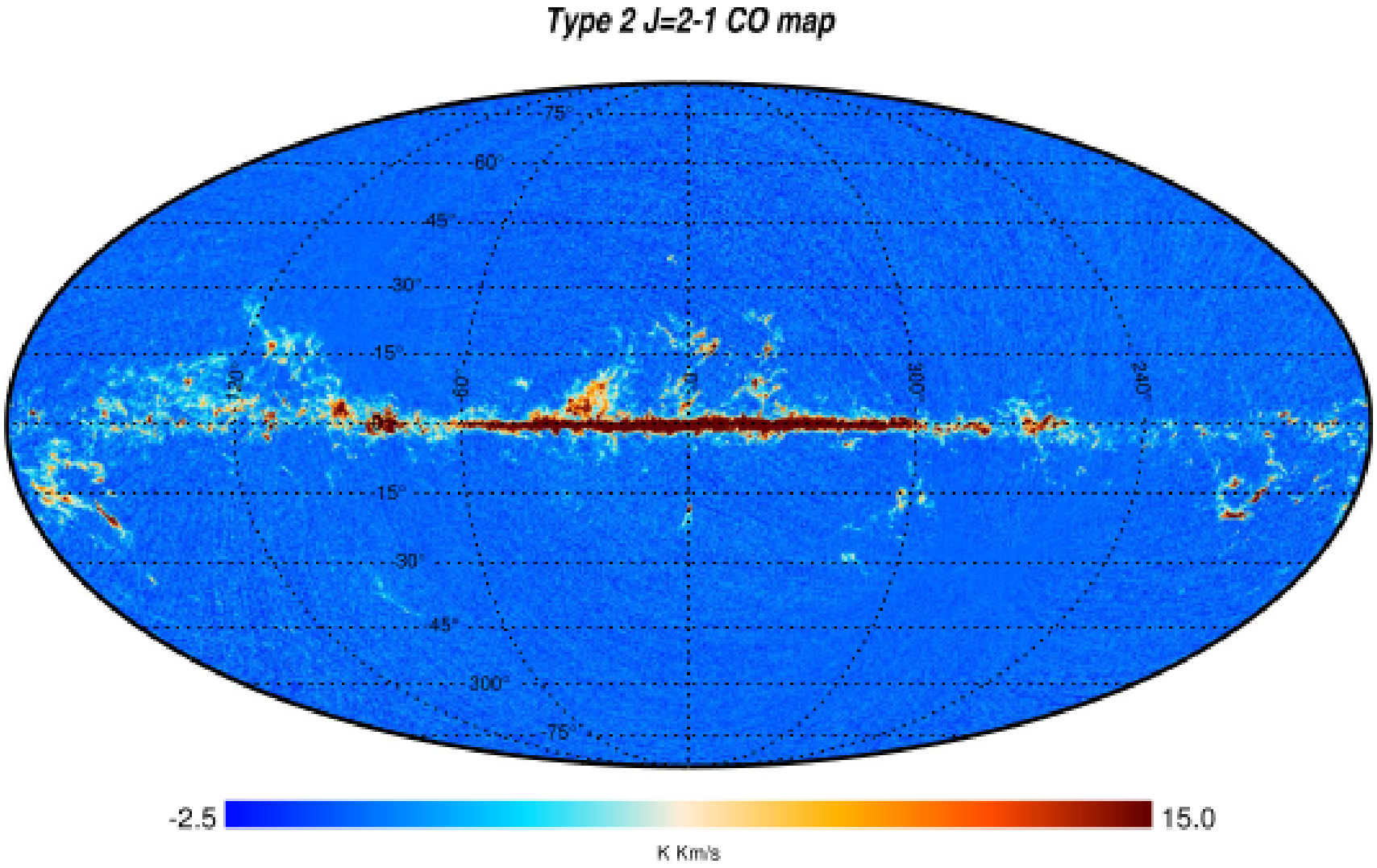

Cold Cores

- We have seen that the dust temperature is of the order of 100 K if it is close enough to a young star.
- In **gas** clouds, the shielding of the outer regions can allow the existence of colder inner regions. Temperatures of ~10 K are reached, with densities $n \sim 10^{4 \div 5}\,\mathrm{cm}^{-3}$.
- These regions are also likely **sites of star formation** (remember that $M_J \propto T^{3/2}$).

Cold Cores

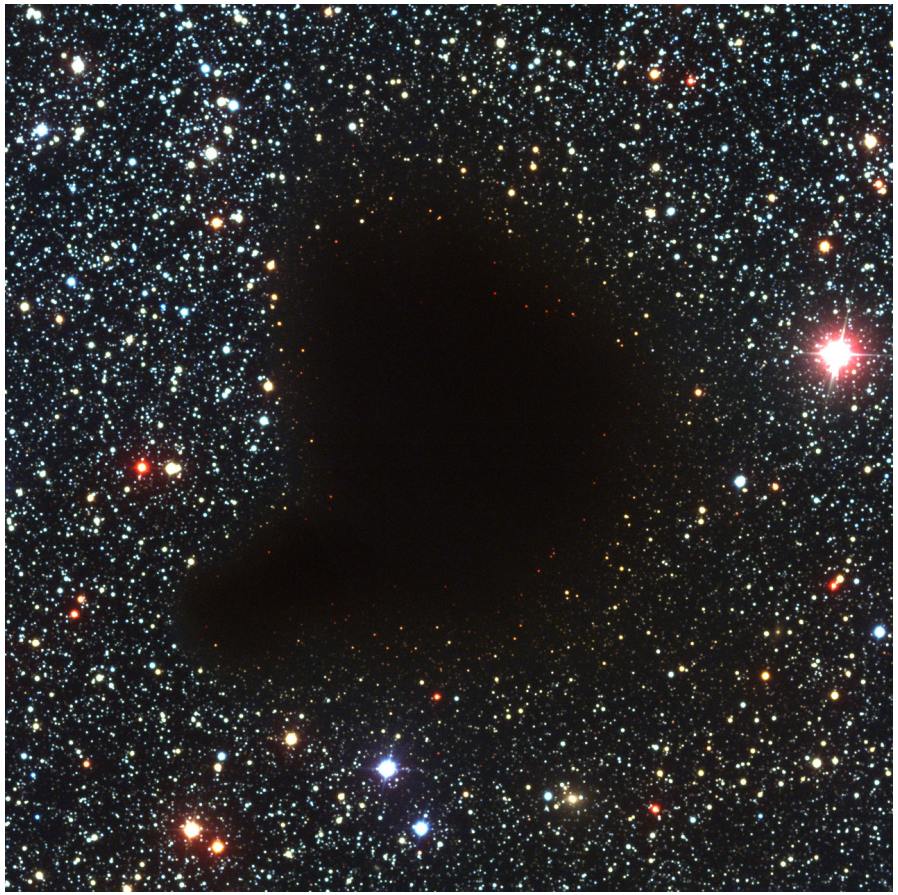

At the center of Barnard 68 («Black cloud») there is a cold core.

HII Regions

HII Regions

- A massive star emits in the visible and in the UV.
- Since to ionize HI it takes $E = h\nu > 13.6\,\mathrm{eV}$ ($\lambda < 91.2\,\mathrm{nm}$), OB stars have the ability to ionize HI.
- When most of the hydrogen is ionized, we speak of **HII regions**.

Strömgren Radius

- OB stars are able to ionize HI only in a region of limited volume. Let's estimate the size of this volume.
- The ionization rate is

$$R_i = N_{\mathrm{UV}},$$

with $[R_i] = \mathrm{ionizations/s}$ and

$$N_{\mathrm{UV}} = \int_{13.6\,\mathrm{eV}}^{\infty} N(\nu)\,\mathrm{d}\nu$$

($N_{\mathrm{UV}} = \mathrm{photons/s}$, if efficiency is 100%).

Strömgren Radius

- The efficiency is likely 100%, because for ionization the cross section is

$$\sigma \sim 10^{-17}\,\mathrm{cm}^2.$$

- For densities $n_H \sim 10^3\,\mathrm{cm}^{-3}$ the mean free path of a photon is

$$\lambda \sim \frac{1}{n_H\,\sigma} \sim 10^{14}\,\mathrm{cm} = 6\,\mathrm{AU},$$

to be compared with the size of HII regions (from 0.1 to 100 pc).

Strömgren Radius

- The recombination rate is

$$R_{\rm rec} = \alpha(T)\, n_e\, n_p\, V = \alpha(T)\, n_p^2\, \frac{4\pi}{3} r_S^3,$$

  with r_S called the **Strömgren radius** and $\alpha(T)$ the coefficient.

- At equilibrium $R_i = R_{\rm rec}$, from which

$$r_S = \left(\frac{3}{4\pi\alpha}\right)^{\frac{1}{3}} N_{\rm UV}^{\frac{1}{3}} n_p^{-\frac{2}{3}}.$$

  Denser HII regions are smaller (typically, $\sim 20\,\mathrm{pc}$).

Strömgren Radius

Given the size R of the cloud, two cases can apply:

1. If $R > r_S$, the cloud is *density bounded*: the HII cloud gradually transitions into the surrounding HI medium;
2. If $R < r_S$, the cloud is *ionization bounded*: the entire cloud is ionized.

Strömgren Radius

- The typical temperature of HII regions is $\sim 10^4\,\mathrm{K}$, compared to the $\sim 100\,\mathrm{K}$ of the surrounding environment. The density, however, shows no discontinuity ($n \sim 10^3\,\mathrm{cm}^{-3}$).
- Other elements are also present in the clouds, each with its own ionization energy. For example:

  1. He: $E_i = 24.6\,\mathrm{eV}$, so HeII regions are less extensive than HII;
  2. C: $E_i = 11.3\,\mathrm{eV}$, so the opposite is true here.

Detecting HII Regions

- The emission of HII regions is due to bremsstrahlung (free-free scattering), with a spectrum

$$T_e \propto \nu^{-\alpha}, \quad \text{with } \alpha \approx 2.1.$$

- Observations reveal that the emission is concentrated on the Galactic plane.

Detecting HII Regions

- One way to distinguish the free-free spectrum from other emissions (e.g., spinning dust) is to correlate it with Hα emission ($n = 3 - 2$, Balmer series).
- Hα is emitted in ionization regions: when an HII (proton) captures an e^-, during de-excitation there is a certain probability ($\sim 50\%$) that the $n = 3 - 2$ transition (Hα) will occur. Therefore Hα signals the presence of ionization.

Detecting HII Regions

Mon. Not. R. Astron. Soc. **341,** 369–384 (2003)

Towards a free–free template for CMB foregrounds

C. Dickinson,★ R. D. Davies and R. J. Davis
Jodrell Bank Observatory, Department of Physics & Astronomy, University of Manchester, Macclesfield, Cheshire SK11 9DL

Accepted 2003 January 16. Received 2002 October 24; in original form 2002 February 15

ABSTRACT

A full-sky template map of the Galactic free–free foreground emission component is increasingly important for high-sensitivity cosmic microwave background (CMB) experiments. We use the recently published Hα data of both the northern and southern skies as the basis for such a template.

The first step is to correct the Hα maps for dust absorption using the 100-μm dust maps of Schlegel, Finkbeiner & Davis. We show that for a range of longitudes, the Galactic latitude distribution of absorption suggests that it is 33 per cent of the full extragalactic absorption. A reliable absorption-corrected Hα map can be produced for $\sim$95 per cent of the sky; the area for which a template cannot be recovered is the Galactic plane area $|b| < 5^\circ$, $l = 260^\circ$–0°–160° and some isolated dense dust clouds at intermediate latitudes.

The second step is to convert the dust-corrected Hα data into a predicted radio surface brightness. The free–free emission formula is revised to give an accurate expression (1 per cent) for the radio emission covering the frequency range 100 MHz–100 GHz and the electron temperature range 3000–20 000 K. The main uncertainty when applying this expression is the variation of electron temperature across the sky. The emission formula is verified in several extended H II regions using data in the range 408–2326 MHz.

A full-sky free–free template map is presented at 30 GHz; the scaling to other frequencies is given. The Haslam et al. all-sky 408-MHz map of the sky can be corrected for this free–free component, which amounts to a $\approx$6 per cent correction at intermediate and high latitudes, to provide a pure synchrotron all-sky template. The implications for CMB experiments are discussed.

Key words: radiation mechanisms: thermal – dust, extinction – H II regions – cosmic microwave background – radio continuum: ISM.

Detecting HII Regions

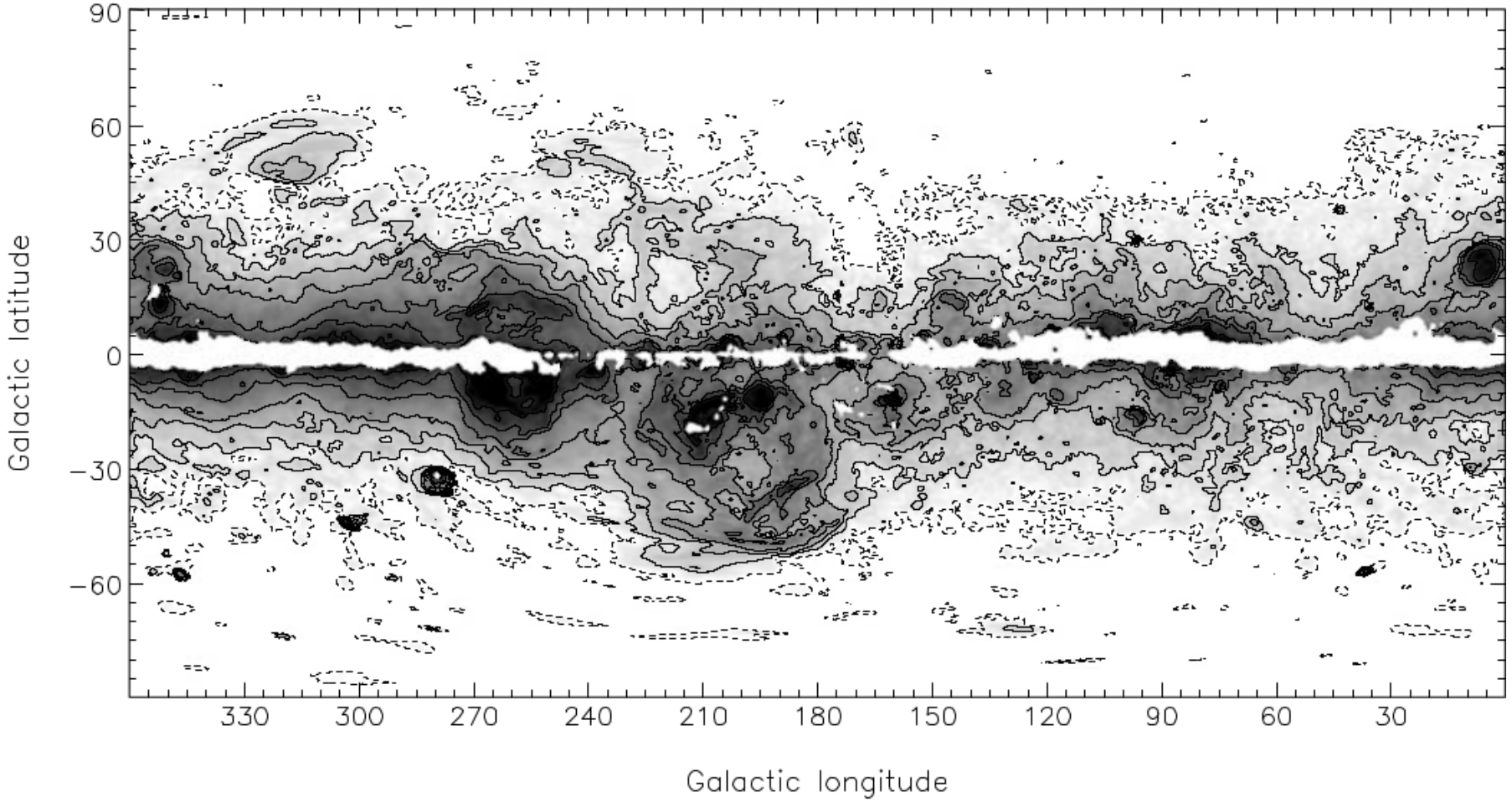

Figure 9. Free–free brightness temperature template at 30 GHz with 1° resolution. Grey-scale is logarithmic from 5 to 1000 μK. Regions where the template is unreliable are masked white. Contours are given at 5 (dot-dashed), 10, 20, 40, 100, 200 and 500 μK.